Ammonia, Methane, Hydrogen Oh My! – Understanding Hazards from Alternative Power to Gas Options

Darren R. Malik, P.E., Senior Engineer – Blast Effects
Baker Engineering and Risk Consultants, Inc., 3330 Oakwell Court, Suite 100, San Antonio, TX 78218 USA

J. Kelly Thomas, PhD, Vice President- Blast Effects
Baker Engineering and Risk Consultants, Inc., 3330 Oakwell Court, Suite 100, San Antonio, TX 78218 USA

The energy and transportation markets are changing substantially as the world rebounds into a post COVID-19 economy. Several major oil companies have announced plans to move beyond their core refining and petrochemical-based business models and become major players in carbon-neutral technologies. Airplane, automotive, and turbine manufacturers are planning to leverage hydrogen and/or ammonia technologies to provide carbon-free options to global markets.

The idea of using hydrogen as a fuel source is not new. Author Jules Verne postulated that in 1874 hydrogen and oxygen would one day be used to "furnish an inexhaustible source of heat and light." NASA used liquid hydrogen as well as hydrogen fuel cell technologies to put a man on the moon over 50 years ago. More recently, industry leaders, regulatory bodies, and research institutions have come together to begin to develop the infrastructure and technological framework required to allow hydrogen to become a significant fuel source.

History has shown that successful market and technology transitions are not guaranteed. Major accidents such as the one that occurred at Three Mile Island (1979) can create a public outcry to ban, or significantly curtail, a given technology, even if accidents do not result in fatalities. Proper understanding of hydrogen and ammonia hazards is one of the key requirements for ensuring public safety and avoiding the derailment of these key components of a carbon neutral economy.

Ammonia and hydrogen represent opposite ends of the spectrum with regard to the potential blast loading resulting from an accidental vapour cloud explosion (VCE), although some in industry have expressed doubts as to whether either of these fuels actually poses a VCE hazard. Ammonia is sometimes discounted as a VCE hazard due to the perceived difficulty in igniting an ammonia-air mixture and/or because of its low laminar burning velocity. Hydrogen is sometimes discounted as a VCE hazard due to the ease with which a hydrogen-air mixture can be ignited and/or because of its buoyancy. This paper discusses these perceptions and presents results from relevant unconfined ammonia, methane, and hydrogen VCE tests.

1 Introduction

Ammonia and hydrogen have both been proposed as potential carbon-free energy carriers that could play pivotal roles in a NetZero carbon future. Both molecules can be synthesized using various processes and energy sources, including "green" pathways using water and electrolysis or plasma technologies (chemeurope.com website) powered by renewable energy sources. Ammonia and hydrogen represent opposite ends of the spectrum with regard to the potential blast loading from an accidental unconfined vapour cloud explosion (VCE). The maximum laminar burning velocity (LBV) of an ammonia-air mixture is in the range of 7 to 15 cm/s (Duynslaegher 2011) while the LBV of a stoichiometric hydrogen-air mixture is on the order of 300 cm/s (NFPA 68 2007).

The Baker-Strehlow-Tang (BST) VCE blast load prediction methodology (Baker et al. 2010, Pierorazio et al. 2005) defines a "low" reactivity fuel as a flammable material having an LBV <45 cm/s and a "high" reactivity fuel as a flammable material with an LBV >75 cm/s. Methane and ethylene are typically used as the "prototypical" low and high reactivity fuels, with LBVs of 40 cm/s and 80 cm/s, respectively (NFPA 68 2007). Thus, the LBV of ammonia is well below the maximum threshold for a "low" reactivity fuel and hydrogen is well above the minimum for a high reactivity fuel.

Relative to more traditional fuels like methane, ammonia and hydrogen occupy "extreme" ends of the fuel reactivity spectrum and warrant special consideration when evaluating their potential to produce an accidental VCE. This paper provides a brief overview of the fundamental concepts required for analyzing VCE events, and then presents the results of unconfined VCE testing performed with ammonia, methane, and hydrogen in congested volumes (Baker et al. 2008).

The tests with ammonia and methane were performed using a worst-case concentration in a highly congested test rig having a length of 72 feet (22 m), a width of 12 feet (3.7 m) and a height of 6 feet (1.8 m). The mixture was ignited against a large wall placed at one end of the rig. The tests with hydrogen were performed in a similar test rig, but with a lower level of congestion (i.e., reduced flame acceleration for a given fuel), a shorter length (48 feet), central ignition (i.e., rather than end ignition), and without the presence of an end wall. The hydrogen tests spanned a range of lean concentrations, from 16% up to 22% hydrogen (vs. a stoichiometric concentration of 30%).

2 Fundamentals of VCE Analysis

At a very high level the hazard created by a combustion-driven event can be categorized by the explosion energy, energy release rate, and stand-off distance to a target of interest. This concept is illustrated via the graphic provided as Figure 1. The simple illustration in Figure 1 shows that while a small candle and a firecracker may be equivalent in size, there is a

fundamental difference between the combustion phenomena of each. If the candle and firecracker were of equivalent energy content, the candle would burn for several minutes while the firecracker would burn in less than a fraction of a second and produce an audible "pop", due to differences in their energy release rates. Of course, these items have relatively low available energy they are not particularly hazardous. The lower energy release rate associated with a large forest fire does not make it inherently less destructive than a large bomb. The key difference between the two is that the bomb releases its energy faster and can rapidly generate a hazardous blast wave and debris field, while the fire may need to burn for days to produce an equivalent level of damage or devastation. However, sufficient separation, potentially miles, should provide a measure of safety from their destructive power.

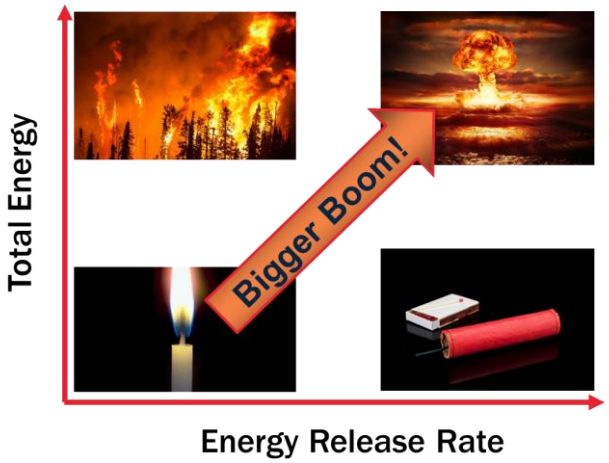

Figure 1. Illustrative Graphic

Decades of research have facilitated the development of various techniques that can be used to evaluate the hazards associated with accidental VCEs. These techniques include simple empirical/curve based models such as the TNO and BST methods, as well as very sophisticated computational fluid dynamics (CFD) models. Regardless of their level of sophistication, these techniques are based on the environment the material is released into as well as the fundamental combustion properties of the flammable materials (e.g., upper and lower flammable limits, LBV, heat of combustion, etc.). Relevant parameters for ammonia, methane and hydrogen are provided in Table 1.

Table 1. Relevant Energy Density and Fundamental Combustion Properties

Parameter	Ammonia	Methane	Hydrogen
Minimum Ignition Energy (MIE) [mJ]	680	0.3	<0.1
Lower Flammability Limit (LFL) [vol%]	15	5	4
Upper Flammability Limit (UFL) [vol%]	28	15	75
Pmax Fuel Concentration [vol%]	23	10	35
Laminar Burning Velocity (LBV) [cm/s]	10	40	312
Heat of Combustion [MJ/m^3]	2.9	3.1	2.6
Gravimetric Energy Density [MJ/kg]	23	54	142
Volumetric Energy Density [MJ/L]	14	22	10

3 Ammonia and Methane Tests

3.1 Test Description

Rig Configuration

The ammonia VCE tests were carried out in a long and highly congested test rig in order to promote flame acceleration and the generation of measurable blast loads. Methane VCE tests were performed in the same rig to provide a basis of comparison with the ammonia VCE tests. The test rig was 72 feet (22 m) long, 12 feet (3.7 m) wide and 6 feet (1.8 m) high. A wall [26 ft. (7.9 m) wide by 16 ft. (4.9 m) high] was placed at the end of the rig, where the flammable mixture was ignited. An isometric

view and photograph of the test rig are provided in Figure 2. With the exception of the wall at the rig end, no other confinement was present within the rig.

The same high congestion level used in the creation of the BST flame speed tables (Baker et al. 2010) was used in these tests. The array was made up of a regular array of vertical cylindrical tubes [2.375-inch (6 cm) diameter, with area and volume blockage ratios of 23% and 5.7%, respectively]. For each 6 ft (1.8 m) cube of space, 61 vertical tubes were installed, along with the 4 solid corner supports. This congestion pattern is intended to be conservative (i.e., highly congested) relative to the congestion in a typical process plant. The location of the ignition source was grade level along the rig centerline near the end wall.

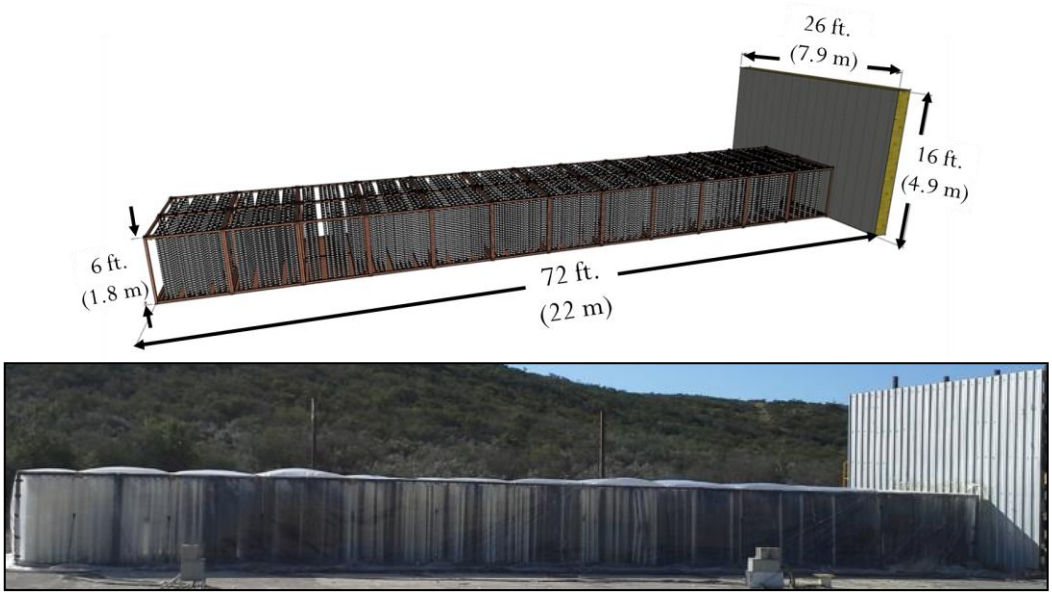

Figure 2. 3D Isometric and Photographic View of Ammonia & Methane Test Rig

Fuel-Air Mixture

The entire test rig was covered in a 1.5 mil (0.0015 in., 0.038 mm) thick plastic sheet, restrained by 12 straps placed along the length of the rig while the fuel-air mixture was generated. The straps were released via remote actuators just prior to ignition to allow the VCE to expand as freely as possible.

Upper and lower fuel concentration acceptance bands were established to minimize the impact of fuel concentration variations. The acceptable concentrations were based on a 1% decrease from the maximum LBV. The target fuel concentration for ammonia tests was 23.2%, with an acceptance range of 22.9% to 23.6% (Duynslaegher 2011). The target fuel concentration for methane tests was 10.0%, with an acceptance range of 9.9% to 10.5%.

The fuel and air were mixed and introduced into the rig through a series of venturis oriented to expel the enriched fuel-air mixture downward. The rig was divided into 3 fuel delivery zones with four venturis each zone in order to support the generation of a uniform fuel-air mixture throughout the rig. Fans were used to circulate the fuel-air mixture in order to quickly achieve a uniform mixture throughout the rig. The fans were positioned at the center of each cube at a height of 5.5 ft. and oriented downward. Each fan was rated for a 110 cfm flow rate, which is equivalent to turning the rig volume over every two minutes. The fans were shut off prior to ignition in order to allow the mixture to reach a quiescent state.

Fuel concentrations were determined indirectly based on oxygen concentration. The oxygen analyzer was calibrated prior to each test using a known concentration of a suitable span gas balanced with nitrogen and with nitrogen as the zero gas. The sample points used to monitor concentration during the test were distributed evenly along the long axis of the rig.

Instrumentation

Blast pressure histories were measured using PCB® Piezotronics general purpose ICP® dynamic pressure sensors (Model CA102B18) connected to a line-powered ICP® sensor signal conditioner using microdot connectors and BNC cables. Each pressure gauge was mounted on a square, ½-inch thick steel plate approximately 12 inches (30 cm) in size. The interior pressure gauges were installed mounted in a recess to reduce the effects of thermal radiation from the fireball. The external gauges were installed with the face of the gauge flush with the top of the mount. The signal from each pressure sensor was recorded using a National Instruments PXIE-1082 Chassis. A schematic of the pressure transducer array is shown in Figure 3; the farthest gauge along a line is at roughly 300 feet from the ignition source location.

Flame propagation was recorded using regular speed high definition and high-speed video. The locations of the high-speed (HS) and high definition (HD) cameras are shown in Figure 3. The high-speed camera was set to record between 500 to 1000 frames per second based on the expected flame speed. The high-definition video was captured at 30 frames per second.

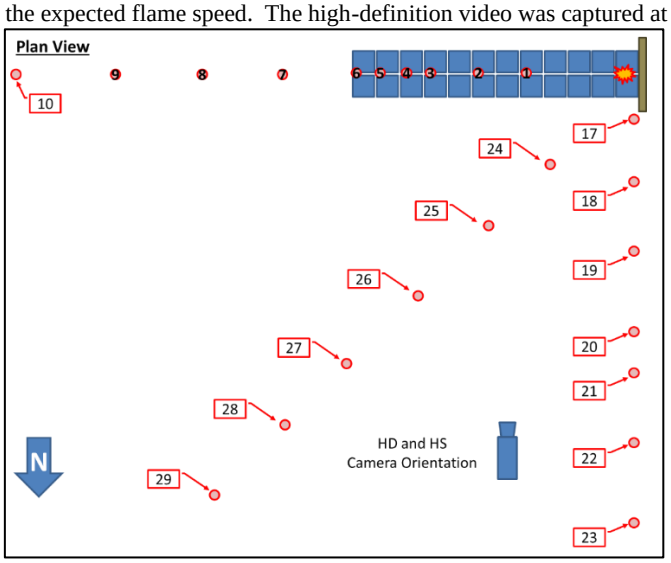

Figure 3. Schematic of the Pressure Transducer Array and Video Cameras

3.2 Results

The measured fuel concentration for each test prior to ignition is provided in Table 2.

Table 2. Fuel Concentrations

Methane		Ammonia	
Test ID	**Concentration (%)**	**Test ID**	**Concentration (%)**
A01	10.0	B01	23.2
A02	10.4	B02	23.0
A03	10.5	B03	23.1

Methane Tests

The measured peak pressures for the long axis gauge lane are provided in Figure 4 as a function of the distance from the ignition location. The test data are shown as points in these figures. The line provided in the figures was generated using BakerRisk's SafeSite$_{3G}$© code with a BST flame speed of Mach 0.19, which was the selected based on a least squares fit of the test data. The location of the end of the test rig is also denoted in this figure.

The observed flame speeds are provided in Figure 5. The maximum and average flame speeds in the rig were approximately 500 ft/s (150 m/s, Mach 0.44) and 350 ft/s (110 m/s, Mach 0.31), respectively. The discrepancy between the observed average flame speed (Mach 0.31) and the least squares fit BST flame speed (Mach 0.19) is due to the test rig aspect ratio, the variance of the flame speed along the length of the rig, and the asymmetric flame propagation (i.e., propagating in a single direction along the rig centerline). The least squares fit BST flame speed of Mach 0.19 under predicts the measured peak pressures in the far field along the direction of flame propagation, but over predicts the measured peak pressures in the far field in the transverse direction.

Ammonia Tests

The ammonia-air tests did not produce measurable overpressures due to the low flame speed developed in these tests. A plot of the observed ammonia-air flame speeds is provided in Figure 6. The flame speeds observed in Tests B01 and B02 were higher than observed in Test B03. A possible explanation for this difference is the wind direction. Tests B01 and B02 were performed with a 5-10 mph (7.3-15 ft/s, 2.2-4.5 m/s) wind blowing in the direction of flame propagation, approximately 30 degrees off the long axis of the rig. Test B03 was performed with a 5 mph wind blowing perpendicular to the direction of flame travel. Correcting Test B01 and B02 for an 8 ft/s (2.4 m/s) flow field along the direction of flame propagation results in the wind corrected ammonia flame speeds shown in Figure 7. The wind adjusted flame speeds for Test B01 and Test B02 are in reasonably good agreement with Test B03. The reason for the higher flame speed in Test B01 near the end of the rig is unknown, but the derivation of flame speed from video at very low flame speeds is subject to increased uncertainty.

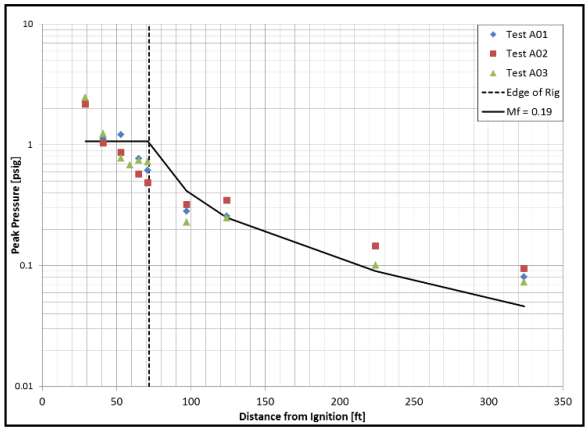

Figure 4. Measured Peak Pressures along the East (long axis) Gauge Lane (methane)

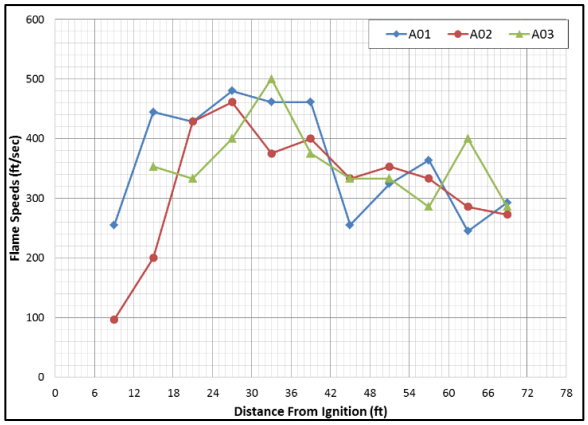

Figure 5. Observed Methane Flame Speeds

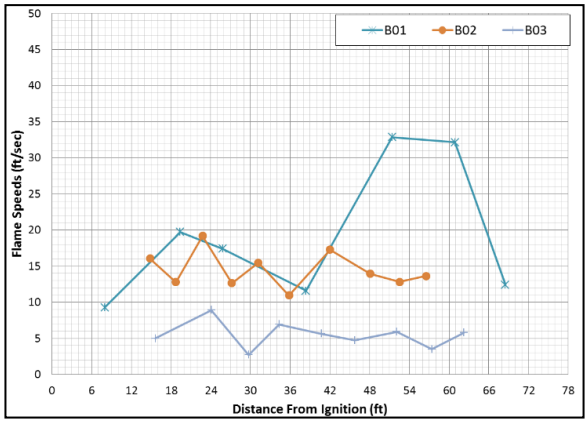

Figure 6. Observed Ammonia Flame Speeds

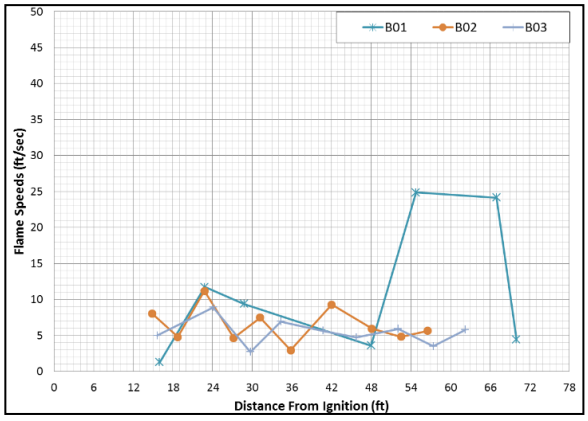

Figure 7. Wind-Corrected Ammonia Flame Speeds

Discussion

The methane-air VCE tests produced maximum blast pressures of approximately 2 psig (0.1 kPa) and maximum flame speeds of approximately 500 ft/s (150 m/s, Mach 0.44). The ammonia VCE tests did not produce measurable overpressures and the observed maximum flame speeds were approximately 25 ft/s (7.6 m/s, Mach 0.02), a factor of 20 lower than in the methane air tests.

An updated BST flame speed table with a new "very low" reactivity class is provided in Table 4 in order to scale the results of this test program for use in a consequence or risk-based facility siting. The values given for the "very low" reactivity fuel class in Table 4 were calculated by multiplying the low reactivity flame speeds by the ratio observed ammonia-air flame speed (Mach 0.02) and the flame speed based on the least squares fit of the methane blast overpressure data (Mach 0.19); even lower values would result if the maximum observed methane flame speed (Mach 0.44) was employed.

Table 4. Updated BST Flame Speed Table with Very Low Reactivity Class

Confinement	Reactivity	Congestion		
		High	Medium	Low
2-D	High	DDT	DDT	0.59
	Medium	1.6	0.66	0.47
	Low	0.66	0.47	0.079
	Very-Low	0.069	0.049	0.008
2.5-D	High	DDT	DDT	0.47
	Medium	1	0.55	0.29
	Low	0.5	0.35	0.053
	Very-Low	0.053	0.037	0.006
3-D	High	DDT	DDT	0.36
	Medium	0.5	0.44	0.11
	Low	0.34	0.23	0.026
	Very-Low	0.036	0.024	0.003

To illustrate the VCE blast loads expected for the "very low" fuel reactivity class, consider a congested volume with a footprint of 200 ft (61 m) by 200 ft (61 m) and a height of 25 ft (7.6 m), which gives a total volume of 1.0×10^6 ft^3 (28,000 m^3). Even if the entire congested volume is treated as high congestion with 2-D confinement (M_f = 0.069), which would be a very extreme

case, the blast overpressure at a standoff from the congested volume center of 150 feet based on the BST VCE blast load prediction method would only be 0.1 psig. Unconfined VCEs of fuels in the "very low" reactivity class (e.g., ammonia) therefore do not appear capable of causing damaging blast loads, even under relatively severe conditions. Similar conclusions are drawn from applying the "Guidance for the Application of the Multi-Energy Method, Second phase"(GAMES) correlation (Mercx, 1998).

4 Hydrogen Tests

4.1 Test Description

Rig Configuration

The test rig for the hydrogen VCE tests was the same as had been previously used by BakerRisk for ethylene VCE testing (Thomas et al. 2003). The rig is similar to that described for the ammonia and methane tests, but the rig was shorter [48 feet (14.6 m)], less congested and did not utilize an end wall. The congestion arrangement was made up of vertical cylindrical tubes [2.375-inch (6 cm) diameter] giving gave a pitch-to-diameter ratio of 4.5 and providing area and volume blockage ratios of 22% and 4.1%, respectively. For each 6 ft (1.8 m) cube, a total of 45 vertical tubes were installed, along with the 4 solid corner supports. This level of congestion corresponds to the "medium" congestion level used in the BST flame speed table (Baker et al. 2010). An illustration and photograph of the test rig in this configuration are shown in Figure 8. The test rig was configured without any confinement (i.e., no wall or roof sections).

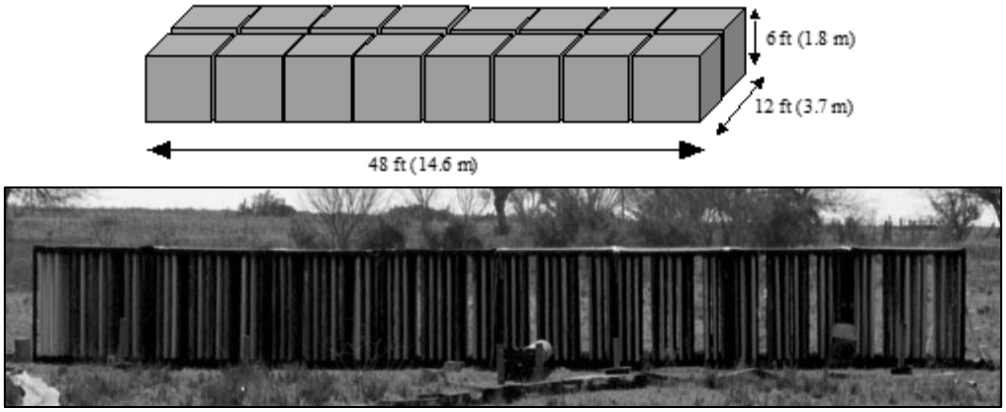

Figure 8. Schematic and Photograph of Hydrogen Test Rig

The hydrogen-air mixtures were developed in essentially the same way as described for the ammonia VCE tests. Six venturis deployed down the length of the rig (mid height) and directed downward were employed to inject the fuel, with additional mixing provided by 16 fans mounted at the top of the rig (1 per cube). The mixture was sampled from 4 different points in the rig to confirm that a uniform mixture at the desired concentration prior to ignition. The fuel was injected over a period of one-half to one hour, and a quiescent period of 5 to 20 minutes was observed prior to ignition. The target hydrogen concentrations for these tests were 16%, 18%, 20% and 22%; all of these mixtures are lean (i.e., stoichiometric concentration is 30%).

The mixture was ignited at the center of the rig near grade level using an electrochemical match. The instrumentation used in these tests was essentially the same as for the ammonia and methane tests (i.e., normal speed video, high speed video and dynamic pressure sensors).

4.2 Results

The measured fuel concentration for each test prior to ignition is provided in Table 4. The pressure histories for monitor point locations external to the rig for Test H02 (18% H_2), Test H04 (20% H_2) and Test H05 (22% H_2) are shown in Figure 9, Figure 10, and Figure 11, respectively. The pressure histories for these three tests at a location 8 feet outside the rig along the long axis are compared in Figure 12. Figure 13 shows the peak blast overpressure as a function of the distance from the ignition location (i.e., rig center). The peak pressures measured within the test rig for all 4 hydrogen tests are summarized in Table 6. A deflagration-to-detonation transition (DDT) occurred in Test H05 at 22% H_2, as evidenced by the large blast pressures measured within the rig as well as flame speeds taken from the HS video.

Table 5. Hydrogen Fuel Concentrations

Test ID	Concentration (%)
H01	16.0
H02	18.1
H04	20.1
H05	22.2

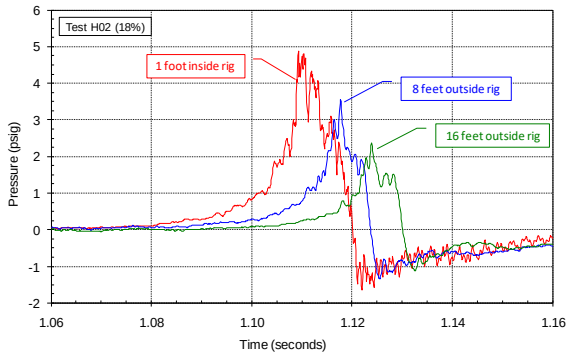

Figure 9. Selected Pressure Histories for Hydrogen Test H02 (18% H_2)

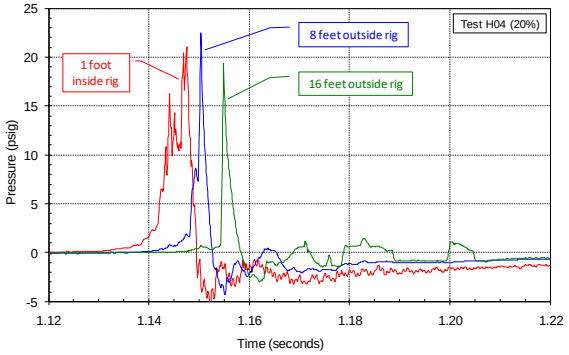

Figure 10. Selected Pressure Histories for Hydrogen Test H04 (20% H_2)

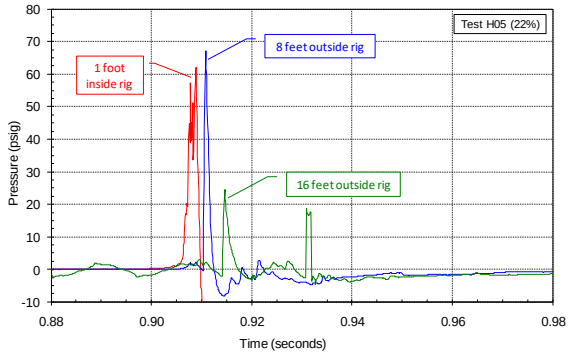

Figure 11. Selected Pressure Histories for Hydrogen Test H05 (22% H_2)

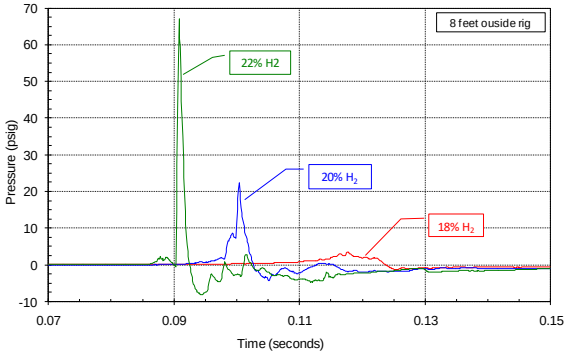

Figure 12. Pressure Histories at 8 Feet Outside Rig (hydrogen)

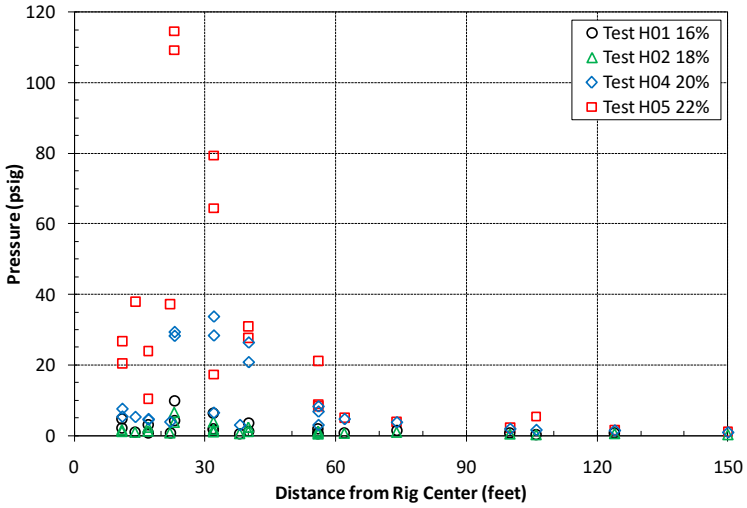

Figure 13. Measured Peak Pressures along Long Gauge Lane (hydrogen)

Table 6. Peak Pressures for Hydrogen Tests

Test ID	Concentration (%)	Equivalence Ratio	Peak Pressure (psig)
H01	16.0	0.44	9.9
H02	18.1	0.51	6.6
H04	20.1	0.58	34
H05	22.2	0.66	115

5 Summary of Findings

The ammonia VCE tests described in this paper clearly demonstrate that damaging blast loads for unconfined ammonia VCEs would not be expected due to the very low LBV of ammonia and the resultant low VCE flame speeds. This is consistent with expectations (Pierorazio et al. 2005, Baker et al. 2008). A "very low" BST flame speed was developed based on these tests. Example blast load calculations show that, even for a relatively severe VCE, damaging blast loads external to a congested volume filled with an ammonia-air cloud would not be expected. It is important to note that the results of the ammonia VCE tests are only applicable to unconfined VCE scenarios. Confined scenarios (i.e., indoor explosions) would behave differently. Testing of confined VCEs with very low reactivity fuels (e.g., ammonia) would be required to define the corresponding explosion hazard, as well as the level of conservatism in the current blast load prediction methodologies for such scenarios. Given the potential for internal vapour cloud explosions to create damaging overpressures, a logical next step would be to perform such tests to better define the explosion hazard associated with such very low reactivity fuels.

The hydrogen VCE tests described in this paper clearly demonstrate that lean hydrogen-air mixtures can undergo a DDT under medium congestion levels even in the absence of confinement. This result was expected based on prior VCE testing performed in the same test rig using ethylene. It should be noted that a detonation, once triggered by a DDT, can propagate through a flammable cloud which extends outside the congested volume, which can dramatically increase the VCE blast load relative to that for a deflagration (Thomas et al. 2013). The potential for a DDT should therefore be considered for release scenarios involving high reactivity fuels (e.g., hydrogen, ethylene, etc.). The data from these tests were used, along with data from the ethylene tests performed by BakerRisk and other data in the literature, to develop DDT evaluation criteria (Thomas et al. 2011). These criteria can be utilized to evaluate the potential for a DDT in actual plant geometries.

6 Implications for Hazard Analyses

Figure 14 provides a plot of LBV and heat of combustion for various fuels, including ammonia, natural gas (methane) and hydrogen. As discussed in Section 2, it is expected that hydrogen would produce significantly larger blast loads than methane and ammonia due to its higher LBV. This agrees with the observations made during the test programs described in this paper.

Moving beyond general rules of thumb to scrutinize the blast hazards associated with low/no-carbon energy carriers (ammonia, methane, and hydrogen) requires the use of software suites that are capable of analyzing the dispersion and interaction of these materials with areas of congestion and confinement that would be present at alternative energy storage/disbursement facilities. BakerRisk's SafeSite©, DNV's Safeti, and Gexcon's Shell FRED software suites are all capable of performing this type of analysis with varying degrees of detail and sophistication. Computational fluid dynamics (CFD) codes can also be used for this purpose.

Blast contours predicted using SafeSite for a generic commercial fueling depot are provided for postulated methane and hydrogen releases in Figure 15 and Figure 16. The assumed release pressures for each material are provided in Table 7. No overpressure contours were predicted for the analyzed ammonia release scenario.

Explosion hazards are not the only hazards associated with ammonia, methane, and hydrogen storage/disbursement systems. The provided blast contours should not be construed to indicate that ammonia is inherently safer than methane or hydrogen as a low/no carbon energy carrier. The potential toxic impacts of an accidental ammonia release are beyond the scope of this paper but should not be neglected when siting an alternative energy storage/disbursement station. It is critical that all stakeholders of the low/no carbon initiatives properly identify and address the risks associated with these technologies. Proponents of these technologies need look no further than the Three Mile Island incident for an illustration of the ability of even a non-fatal incident to grab public attention and revoke public acceptance of a technology. All of the current effort and excitement surrounding a NetZero world could evaporate if industry fails to continually deliver a record of safe (i.e., low-risk) operations.

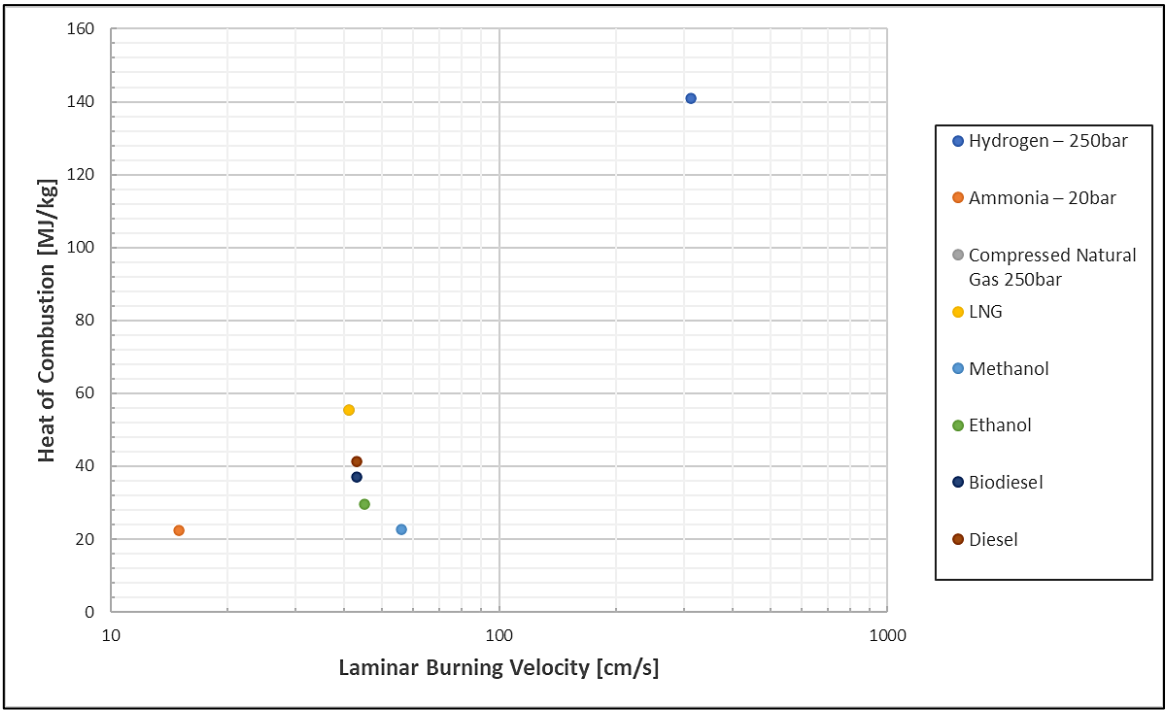

Figure 1 LBV and Heat of Combustion

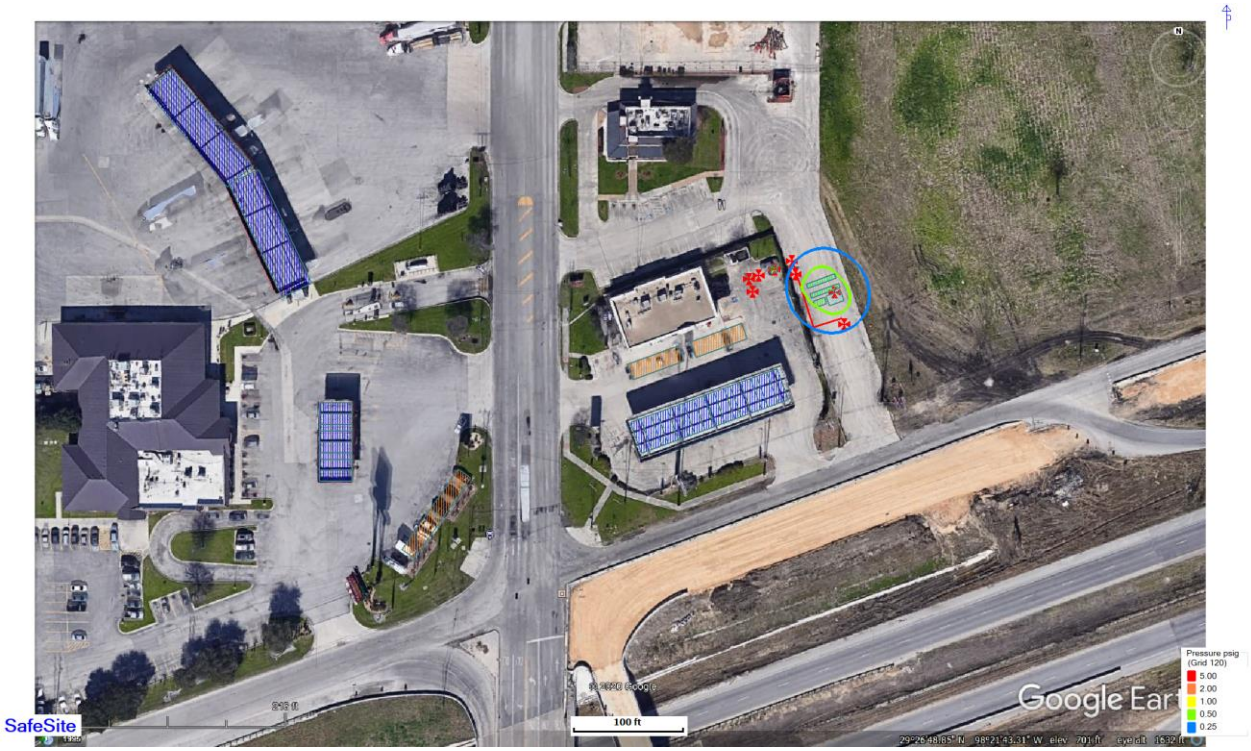

Figure 2. SafeSite predicted blast contours for a postulated 2-inch LNG release

Figure 3. SafeSite predicted blast contour for a postulated 2-inch LH_2 release

Table 1. Modeled Storage/Release Conditions

Material	Temperature [°F]	Pressure [psig]
Ammonia	70	125
Methane	-260	3
Hydrogen	-408	90

7 Acknowledgements

The ammonia and methane tests were performed under the sponsorship of Honeywell International, Inc., and their support is gratefully acknowledged. Brad Horn, Jef Rowley, Martin Goodrich, Austin Burch and Emeka Ugwu were instrumental in the completion of those tests and their contribution to this work is also gratefully acknowledged (Downes, 2016).

The hydrogen tests were performed as a BakerRisk Internal Research program; the support of Martin Goodrich and Robert Duran in performing those tests is gratefully acknowledged (Thomas, 2014).

8 References

1. The new alchemy in carbon neutrality: turning water into ammonia with only renewable energy! (chemeurope.com)
2. Duynslaegher, Catherine (2011) "Experimental and Numerical Study of Ammonia Combustion" Université catholique de Louvain. Sept. 2011.
3. National Fire Protection Association (2007) Standard on Explosion Protection by Deflagration Venting (NFPA 68), Quincy, MA.
4. Baker, Q.A. et al. (2010) Guidelines for Vapor Cloud Explosion, Pressure Vessel Burst, BLEVE and Flash Fire Hazards, 2nd Edition, AIChE CCPS & John Wiley and Sons, New York, NY.
5. Pierorazio, A.J., J.K. Thomas, Q.A. Baker and D.E. Ketchum (2005) "An Update to the Baker-Strehlow Tang Vapor Cloud Explosion Prediction Methodology Flame Speed Table," Process Safety Progress, 24(1): 59-65.
6. Baker, Q.A., K.A. Dejmek and X. Qin (2008) "Facility Siting in Ammonia Facilities," AIChE 53rd Annual Safety in Ammonia Plants and Related Facilities Symp., Paper 3e, San Antonio, TX, Sept. 9, 2008.
7. Factory Mutual Global, Property Loss Prevention Data Sheets, 7–42, "Guidelines for Evaluating the Effect of Vapor Cloud Explosions Using a Flame Acceleration Method," Oct. 2008.
8. Thomas, J.K., C.D. Eastwood and M.L. Goodrich (2015) "Are Unconfined Hydrogen Vapor Cloud Explosions Credible?" Process Safety Progress, 34(1): 36-43 (presented at AIChE 10th Global Congress on Process Safety / 48th Loss Prevention Symposium, New Orleans, LA, Mar 30-Apr 2, 2014).
9. Downes, A.M., S. Rogers, D.R. Malik and J.K. Thomas (2016) "Ammonia VCE Testing and Implications for FSS Consequence Analyses and Risk Assessments," AIChE 12th Global Congress on Process Safety (50th Loss Prevention Symposium), Houston, TX, April 11-13, 2016.
10. Thomas, J.K., R.J. Duran and M.L. Goodrich (2010) "Deflagration to Detonation Transition in a Lean Hydrogen-Air Unconfined Vapor Cloud Explosion," Mary Kay O'Connor Process Safety International Symposium," College Station, TX, October 27, 2010.
11. Mercx, W.P.M., A.C. van den Berg. And D. van Leeuwen (1998) Application of Correlations to Quantify the Source Strength of Vapour Cloud Explosions in Realistic Situations, Final Report for the project: 'GAMES', TNO Prins Maurtis Laboratory.
12. Thomas, J.K., A.J. Pierorazio, M. Goodrich, M. Kolbe, Q.A. Baker and D.E. Ketchum (2003) "Deflagration to Detonation Transition in Unconfined Vapor Cloud Explosions," Center for Chemical Process Safety (CCPS) 18th Annual International Conference & Workshop, Scottsdale, AZ, 23-25 September 2003.
13. Thomas, J.K., M.L. Goodrich and R.J. Duran (2013) "Propagation of a Vapor Cloud Detonation from a Congested Area into an Uncongested Area: Demonstration Test and Impact on Blast Load Prediction," Process Safety Progress, 32(2): 199-206 (presented at AIChE 8th Global Congress on Process Safety / 46th Loss Prevention Symposium, Houston, TX, April 1-5, 2012).
14. Thomas, J.K., J. Geng and C.D. Eastwood (2011) "Comparison of Deflagration to Detonation Transition (DDT) Criteria for With Test Data from Unconfined Ethylene-Air Vapor Cloud Explosion," AIChE 7th Global Congress on Process Safety (45th Annual Loss Prevention Symp.), Chicago, IL, March 13-16, 2011.